JP0555023

Experimental study of particle transport and density fluctuation in LHD

K.Tanaka1) , C. Michael1), A. Sanin1), L.N. Vyacheslavov1), K.Kawahata1), S. Murakami3), A. Wakasa4) , H. Yamada1), J. Miyazawa1), S. Morita1), T. Tokuzawa1), T.Akiyama1), M.Goto1), K. Ida1), M. Yoshinuma1), I.Yamada1), M. Yokoyama1), S. Masuzaki1), T. Morisaki1), R.Sakamoto1), H.Funaba1), A.Komori1) and LHD experimental group

1)National Institute for Fusion Science, 322-6 Oroshi, Toki, 509-5292, Japan
2)Budker Institute of Nuclear Physics, 630090, Novosibirsk, Russia
3)Department of Nuclear Engineering, Kyoto University, Kyoto 606-8501, Japan
4)Graduate School of Engineering, Hokkaido University, Sapporo, 060-8628, Japan

e-mail contact of main author: ktanaka@LHD.nifs.ac.jp

Abstract. A variety of electron density (n_e) profiles have been observed in Large Helical Device (LHD). The density profiles change dramatically with heating power and toroidal magnetic field (B_t) under the same line averaged density. The particle transport coefficients, i.e., diffusion coefficient (D) and convection velocity (V) are experimentally obtained in the standard configuration from density modulation experiments. The values of D and V are estimated separately in the core and edge. The diffusion coefficients are found to be a strong function of electron temperature (T_e) and are proportional to $T_e^{1.7 \pm 0.9}$ in the core and $T_e^{1.1 \pm 0.14}$ in the edge. Edge diffusion coefficients are proportional to $B_t^{-2.08}$. It is found that the scaling of D in the edge is close to gyro-Bohm-like in nature. Non-zero V is observed and it is found that the electron temperature gradient can drive particle convection, particularly in the core region. The convection velocity in the core reverses direction from inward to outward as the T_e gradient increases. In the edge, convection is inward directed in most cases of the present data set. It shows a modest tendency, being proportional to T_e gradient and remaining inward directed. However, the toroidal magnetic field also significantly affects the value and direction of V. The density fluctuation spectrum varies with heating power suggesting that it has an influence on particle transport. The value of $k_\perp \rho_i$ is around 0.1, as expected for gyro-Bohm diffusion. Fluctuations are localized in both positive and negative density gradient regions of the hollow density profiles. The fluctuation power in each region is clearly distinguished having different phase velocity profiles.

1. Introduction

Particle transport of bulk ions and electrons is one of the most important issues of magnetically confined plasma research. However, compared with energy transport study, fewer works have been done. This is because of the difficulties of the experimental estimation of the particle source and the existence of the convection term in the particle balance equation. These make estimation of particle transport coefficients, i.e., diffusion coefficients (D) and convection velocity (V) impossible from simple particle balance analysis in the equilibrium state. Large Helical Device (LHD) is a large heliotron whose operational envelope extends towards the fusion relevant regime. Although thermal transport has been discussed in many reports, this is the first systematic study of the bulk ion and electron particle transport in LHD. The diffusion coefficients and convection velocities are separately estimated from the propagation of periodically modulated density by controlling the gas puff.

In most of the operational regimes of LHD, particle transport is dominated by anomalous transport. Therefore, experimental study of the turbulence is also important. In this paper, characteristics of electron density fluctuations, which can play a role on particle confinements, are also described.

2. Density profiles in LHD

The density profiles in LHD change with the magnetic configuration, magnetic field strength, and heating power. This is because the characteristics of particle transport are determined by these experimental conditions. Figure 1 show T_e and n_e profiles at different neutral beam injection (NBI) heating power. The magnetic configuration is the so-called standard configuration, whose magnetic axis position (R_{ax}) is 3.6m. This configuration has the largest plasma volume and achieves the highest stored energy and best energy confinement improvement [4].

As shown in Fig.1 (a), T_e increases with increasing heating power. The shape of the T_e profiles remains parabolic and peaked at the center almost regardless of the heating power. On the other hand, n_e profiles change dramatically from peaked one to hollowed one with increase of the heating power. The value of n_e is non-zero at the last closed flux surface (LCFS), which is labeled as having a normalized radius ρ equal to 1, although T_e is almost zero at this position. This is due to the existence of an ergodic region, which has finite connection length and located outside of LCFS. The plasma can be confined in this ergodic region. It is known from measurements of the spatial profile of H_α radiation that the peak of particle source is always located outside of LCFS surface when n_e at $\rho = 1$ is higher than $1x10^{18}m^{-3}$. In addition, particle fuelling from NBI is negligible in these cases. Therefore, the distinction between n_e profiles in Fig.1 (b) is not due to the difference of the particle source deposition but due to the dissimilarity in the transport. The density profiles also vary with magnetic configuration. At similar collision frequencies, the n_e profiles tend to become more hollow as R_{ax} increases [5]. In this paper, we concentrate only on the dependence of particle transport on heating power and B_t in standard configuration. The heating scheme used is NBI, whose power is scanned from 1MW to 8.5MW in this series of experiments. The line averaged density is almost kept constant to be free from the density dependence of the particle transport. Investigated plasmas lie in the plateau and so-called $1/\nu$ region, where helical ripple transport is enhanced. The normalized collisionality ($\nu^*_h = \nu_{ei} qR / \varepsilon_{h,eff}^{1.5} v_{th}$) is 0.26~2.6 at ρ=0.75. The gas species is hydrogen.

3. Density Modulation Experiments in LHD

The particle flux can be written as the sum of diffusion and convection terms as follows:

$$\Gamma = -D\nabla n_e + n_e V \,. \tag{1}$$

The particle balance equation is the following:

$$\frac{\partial n_e}{\partial t} = -\nabla \cdot \Gamma + S = -\frac{1}{r}\frac{\partial}{\partial r} r\Gamma + S \,. \tag{2}$$

Here, S is a particle source rate. If the particle source, which is located at the edge, is modulated, the density perturbation propagates from the edge to the core. The parameters D and V characterize this propagation. From the analysis of modulated components, D and V can be determined independently of the absolute value of the particle source [6], which is difficult to estimate experimentally. For this analysis, the source profiles (only relative shape) from 1-D calculations of the neutral penetration [7] are used.

Figures 2 (a) and (b) show the amplitude and phase profiles of line-integrated measurements for two discharges measured by the multi channel far infrared interferometer [2]. Modulation frequencies of 2, 5 and 10Hz are chosen to get several periods during the density flat top interval to ensure accurate measurements of phase and amplitude. A 5 Hz modulation was applied for the 5.2 MW heating case and 2 Hz modulation was applied for the 1 MW heating case. When core diffusion is lower, modulations cannot reach the core region

and results become insensitive to core transport. Modulations at lower frequency can penetrate deeper in the core. At lower heating power the diffusion is smaller as described in next section. So for the low diffusion case, a 2 Hz modulation was employed to estimate core diffusion coefficients. The modulation amplitude is kept less than 4 % of line averaged density in order to avoid modification of the underlying transport.

The modulated part of particle balance equation can be expressed in cylindrical geometry by the following equation:

$$\frac{\partial^2 \tilde{n}_e}{\partial r^2} + \left(\frac{1}{r} + \frac{1}{D}\frac{\partial D}{\partial r} - \frac{V}{D} \right) \frac{\partial \tilde{n}_e}{\partial r} - \left(\frac{V}{rD} + \frac{1}{D}\frac{\partial V}{\partial r} \right) \tilde{n}_e - i\frac{\omega}{D}\tilde{n}_e + \frac{\tilde{S}}{D} = 0. \quad (3)$$

Here, tilde symbols indicate modulated components; ω indicates modulation frequency. The n_e tilde is complex function, which has both amplitude and phase information. The D and V are obtained from the fitting the solution of Eq. (3) to experimental data. Since the interferometer measures line integrated quantities, line-integrals of solutions to Eq. (3), parameterized by D and V, are fitted to the measured data.

Figure 2 shows examples of integrated modulation amplitude and phase at different heating power. A clear difference is observed between two cases. The amplitude and phase are calculated by the correlation analysis. The error bar is the uncertainty of the determination of phase and amplitude. The amplitude and phase profiles are calculated using model profiles of D and V as shown in Fig.3. Because the core and edge transport can be different, two fitting variables for both D and V are used. One is the core value (D_{core}, V_{core}) and the other is edge value (D_{edge}, V_{edge}). The profiles of D are assumed to be constant in the core and edge and change at $\rho = 0.7$. The value of V is zero at $\rho = 0$ and V profiles are assumed to vary linearly with ρ, changing slope at $\rho = 0.7$. The values of V at $\rho = 0.7$ and $\rho = 1.0$ are taken to represent V_{core} and V_{edge} respectively. The transition points of D and V are fixed at $\rho = 0.7$ in this series of analysis in order to make fitting more stable. As shown in Fig.2, measurements and calculation agree reasonably. The estimation errors of D and V in Fig.3 originate from estimation inaccuracy of modulation amplitude and phase.

4. Characteristics of transport coefficients

4.1 Particle Diffusion

As shown in Fig. 3 (a), the D is higher in the core than in the edge for both cases. Figure 4 shows the profile of electron thermal diffusion coefficients χ_e obtained from power balance analysis by using PROCTR [7] code. Typically, the χ_e profiles also show larger values in the core as well in LHD at standard configuration [5]. The predominance of core value of D and χ_e was also observed in this series of modulation experiments. The lower values of D and χ_e in the edge region are the reason for the steep edge gradients of n_e and T_e, which is observed in Fig.1 (a) and (b). The strong magnetic shear may play a role to stabilize microinstabilities and reduce diffusion in the edge region. The value of χ_e is around one order magnitude larger than D. This is similar to the case of typical tokamak experiments.

A comparison of the experimentally determined D with a neoclassical estimate, calculated by the DCOM [9] code is presented in Fig. 5. In both cases, the experimental value is one order of magnitude larger than the neoclassical estimate. The diffusive particle flux is predominantly anomalous. This suggests that microturbulence plays an important role on diffusive flux.

The temperature dependence of D forms the basis for the investigation of the anomalous transport model. For Bohm-like diffusion, where particle transport is influenced by the long-wavelength fluctuations (up to plasma minor radius), D is proportional to T_e, while for gyro-Bohm-like diffusion, where short-wavelength fluctuations (around the ion gyro-radius) play a role, D is proportional to $T_e^{1.5}$. For this investigation, a systematic scan of NBI heating power (P = 1~8.5MW) keeping background density almost constant ($n_{e\text{-}bar}$ = 1.2 ~ 1.5x10^{19}m^{-3}) is carried out at R_{ax} = 3.6m. The data set contains discharges at B_t = 2.8 and 2.75T. The small difference of B_t is not expected to affect the transport.

Figure 6 shows the T_e dependence of D_{core} and D_{edge}. The electron temperature in Fig.6 is the averaged value within ρ = 0.4 ~ 0.7 for the core and ρ = 0.7 ~ 1.0 for the edge. The data set include 2, 5, and 10Hz modulation frequencies. When core diffusion coefficients cannot be determined from fitting because of lower diffusion or higher modulation frequency, a spatially constant D was assumed. Then, the estimated D was taken as D_{edge}, because the analysis has sensitivity in the edge region in this case. The diffusion coefficient increases with T_e both in the core and edge regions. The fitted power-law scaling of the observed T_e dependences are $D_{core} \propto T_e^{1.7\pm0.9}$ and $D_{edge} \propto T_e^{1.1\pm0.14}$. The difference of the T_e dependence in the core and edge suggests the existence of different types of turbulent transport in the core and edge. From the T_e dependence, D_{core} is gyro Bohm like rather than Bohm like. However, for the edge region the distinction between the two models is not as clear.

4. 2 Particle Convection

Hollow density profiles are observed in LHD in many discharges. This is a harsh contrast to tokamak plasmas, where most density profiles are peaked. As is shown in Fig.1, density profiles become hollow with an increase of T_e. The hollow density profiles clearly indicate the existence of the outward convection, because the particle source, which is localized out of LCFS, cannot maintain the hollow density profiles. In addition, density modulation experiments can estimate D and V separately, and results of many experimental discharges show an existence of the particle convection, which is the second term of Eq.(1). This fact suggests that off-diagonal terms of transport matrix contribute to the total particle flux. For example, to sustain the positive density gradient, which is observed at ρ = 0.6 ~ 0.9 in 8.5MW heating case (see Fig.1(b)), in the equilibrium sate, off-diagonal transport coefficients should determine the particle flux, since diffusion does not contribute to total particle flux in this region. The next question is which driving term or which gradient determines convective flux.

The change of the n_e profile in Fig.1 (b) suggests a correlation between V and T_e gradient. Figure 7 shows the T_e gradient dependence of V. The value of V at ρ = 0.7 is considered to be V_{core}, and V_{edge} is considered to be the value at ρ =1.0. The electron temperature gradient is the averaged over the region ρ = 0.4 ~ 0.7 for core and ρ = 0.7 ~ 1.0 for the edge. The edge convection is inward directed in the most cases. On the other hand, V_{core} changes direction from inward to outward with increasing of T_e gradient. The temperature gradient dependence of V_{edge} is not very clear although there is a modest tendency of decreasing V_{edge} with increasing T_e gradient. The dependence of V_{core} on T_e gradient is more pronounced. The core convection velocity shows a clear dependence on T_e gradient. Comparison with theoretical model of convection based on turbulence [10] is necessary for further understanding of the convection term.

4.3 The Effects of the Toroidal Magnetic Fields

The effect of B_t can give more clear remarks about whether diffusion is Bohm-like (D is proportional to B_t^{-1}) or gyro-Bohm-like (D is proportional to B_t^{-2}). The modulation experiments were done to study the effect of B_t on D and V. A comparison is made between two discharges at different B_t (1.49 and 2.75 T). In order to be free from the n_e and T_e dependence of D and V, the heating power and gas fuelling were adjusted to produce almost identical T_e profiles and similar line averaged density. The profiles of T_e and n_e are shown in Fig.8. The results for the estimated D and V are summarized in table.1. Since a relatively high modulation frequency of 10Hz was used to make the analysis possible during the short density flat top (~1sec), a constant D profile, which mostly represents the edge value, is used for this analysis. The B_t dependence of D, which characterize the edge value is $Bt^{-2.08}$, which is very close to gyro-Bohm diffusion. Considering the T_e dependence ($D_{edge} \propto T_e^{1.1\pm0.14}$), the edge diffusion is gyro-Bohm-like rather than Bohm-like. The gyro-Bohm nature is the same that of thermal diffusivity [4].

The effects of B_t is also seen in the character of the particle convection. At B_t = 1.49T, a strongly hollow profile was observed as shown in Fig.8 (b) and corresponding to this, the estimated V_{core} is outward directed. On the other hand, at B_t = 2.75T, flat density profiles are recorded as shown in Fig.8 (b) and the convection was observed to be inward directed in both the core and edge. As described in Section 4.2, the temperature gradient has clear correlation with V_{core}. However, the results in table 1 and Fig.8, indicate T_e gradient is not only parameter which drive core convection. For further investigation, the NBI power was scanned and modulation experiments were done at B_t = 1.5T.

Figure 9 shows comparison of T_e gradient dependence of V_{core} at low field (B_t = 1.5T) and high field (B_t = 2.75 and 2.8T). The dataset at high field is the same data as one in Fig.7. The modulation frequency of the data set at low filed was 2.5 and 5Hz. Because of the high recycling, averaged density could not be kept constant in this series of experiments. The density varies from 1.8 to $5.0\times10^{19}m^{-3}$ in the dataset at low field of Fig.9. As shown in Fig.9, at the same T_e gradient, the core convection tends to be higher and outward directed at lower field. Although the density dependence of V_{core} has to be kept in mind, the core convection reverses direction at higher T_e gradient at higher B_t.

5. Characteristics of Turbulence

As shown in Fig.5, diffusion is dominated by anomalous terms. To get a comprehensive picture of particle transport, it is necessary to measure microturbulence. The spectrum and spatial structure of fluctuations, dependence on the parameters of the discharge and correlation with transport characteristics can provide ideas to understand anomalous transport. In LHD, microturbulence was measured by using a CO_2 laser Phase Contrast Imaging (PCI) Interferometer [11,12,13]. Since the length of scattering volume for the expected wavenumber region is larger than the plasma size for the 10.6μm infrared CO_2 laser wavelength, no spatial resolution is expected along beam axis. However, by using strong magnetic shear of LHD, it is possible to get modest spatial resolution along the probe beam [14].

5.1 Spectrum Structure

The qualitative difference of the fluctuation spectra is observed at different NBI heating powers using PCI with 32-channel one-dimensional linear detector array. Figure 10 shows wavenumber (k) and frequency (f) spectra, which are measured by PCI at different heating power and similar line averaged densities. Spatial localization around the minor

radius was achieved by tilting the image of the detector array in plasma. The magnetic field shear is very strong in LHD. The field pitch angle reaches 40 degrees at the last closed flux surfaces compared with the zero angle in the plasma centre. The parallel wavenumber of fluctuations is much smaller than the perpendicular one. If the axis of one-dimensional detector array is set to be perpendicular to the particular magnetic field, only projections of fluctuations on the axis are recorded. The projected wavenumber at some other location becomes smaller as magnetic field direction is getting closer to the array axis, then contribution of signal decreases when projected wavenumber reaches the instrumental cut-off wavenumber. The axis of the linear detector image was set to be perpendicular to the magnetic field near upper last closed flux surfaces. Then signal is weighted here with a resolution around minor radius.

The measurements range of wavenumber and frequency ranges are k = 0.1 ~ 1.25mm^{-1} and f = 5 ~ 125kHz respectively. The measured wavenumber is comprised mostly of poloidal components. The peak wavenumber is 0.2 mm^{-1} at 1MW heating and 0.3 mm^{-1} at 6.5 MW heating. The value of $k_{\perp}\rho_i$ is around 0.1, which is roughly equal to that expected for the gyro-Bohm diffusion model. In both case, fluctuation propagate in the electron diamagnetic direction in the laboratory frame.

As observed in Section 4.1, higher heating power causes larger diffusion. This observation can be compared with the properties of the fluctuations. As the diffusion coefficient is proportional to (step size)^2/(step time), the anomalous component can be expressed as the (eddy size)^2/(eddy turnover time)~(frequency width)/(wave number)^2. As shown in Fig.10, broad spectra in k are observed and the value of k at the peak of the wavenumber spectrum is reduced and the frequency spectrum is broadened at higher heating power. The change of the spectrum is qualitatively consistent with enhanced diffusion at higher heating power. The measured wavenumber is poloidal components, although radial components are more essential for transport. The shifting of peak wavenumber of radial components to lower values, when energy confinements degrade at lower B_t, is also observed in LHD [11]. Since the change in frequency spectrum width in Fig. 10 can be partly due to the increase of plasma rotation, simultaneous measurements of E_r or radial wavenumber-frequency spectrum, which is free from plasma rotation effects are necessary for more detailed discussion.

As shown in Fig.10, total fluctuation power is not very different or even slightly smaller at higher heating power, where diffusion is enhanced. This suggests that the fluctuation intensity is not the only parameter characterizing anomalous particle transport

5.2 Spatial Structure

Recently, a new technique was developed to measure spatial profile of fluctuations [12, 13]. By using a 48 (6 by 8) channel two-dimensional detector, it is possible to get fluctuation profile from single shot and single time by taking advantage of the strong magnetic shear. The one-dimensional PCI, which is described in the previous section, measures projected fluctuation picture to the axis of the array, which are integrated within measurements volume. The two dimensional PCI (2D PCI) records 2-D fluctuation picture integrated along injected beam direction as shown in Fig.11. This two-dimensional picture contains fluctuations propagating perpendicular to magnetic field lines, along the path of the probe beam. The propagation direction can be resolved by the spatial two-dimensional Fourier transform. The location of fluctuation can be determined from the position of the field, which is perpendicular to propagation direction.

The spatial profile of fluctuation power spectrum was measured by using 2D-PCI for k = 0.5 ~ 1.5mm^{-1} and f = 5 ~ 500 kH. Figure 12 shows T_e and n_e profiles of target of the

measurements. The magnetic configuration is standard configurations (R_{ax}=3.6m), which is the same as ones analyzed in section 2 ~ 4 and B_t is 2.75T. A peaked T_e and hollowed n_e profiles are observed as shown in Fig. 12. The density modulation was done for this discharge and shows outward convection in core, which is 0.24 m/sec at ρ = 0.8 and inward convection at edge, which is -0.54 m/sec at ρ = 1.0. The diffusion coefficient was estimated to be 0.05m^2/sec with spatially constant model.

Figure 13 shows contour plotting of the spectrum intensity in ρ-phase velocity space from laboratory frame. Maximum Likelihood Method (MLM) was applied to get fine spectrum resolution [15]. The maximum likelihood method has an advantage of fine spectrum resolution, but there are some uncertainties of the spectrum intensity. The several structures can be clearly seen in Fig.13, however, the intensity of each structure contains estimation error due to the nature of MLM.

Since fluctuations along beam axis in Fig.11 contribute to the signal, fluctuations from upper and lower of equatorial plane can be distinguished. The spectrum in positive and negative ρ region corresponds to top and bottom part of measured cross section in Fig.11. The poloidally rotating fluctuation as shown with blue arrow in Fig.11 have opposite direction in the top and bottom, therefore, poloidally rotating fluctuation components have a opposite sign in top and bottom region.

Asymmetries between top and bottom region is observed, however, the structures are similar in both regions. The spectrum consists of two parts. One is localized in positive gradient region, where $|\rho| \le 0.9$, the other is localized in negative density gradient region, where $|\rho| \ge 0.9$. The phase velocity of the positive density gradient mode is close to E_rxB_t poloidal rotation velocity with green lines in Fig.13. The radial electric field is calculated from ambipolar condition of neoclassical theory by GASRAKE code [16] with measured T_e and n_e profiles of Fig.12. The calculated E_r from neoclassical ambipolar condition reasonably agrees with measured E_r by charge exchange spectroscopy [17], which is not available in the discharge of Fig.12 and Fig.13.

On the other hand, spatial structure of the negative density gradient mode is complicated. Both electron and ion diamagnetic propagating components are observed. Presence of both electron and ion diamagnetic components, which is clearer in the bottom part, can be interpreted as an existence of strong velocity shear. The blue lines in Fig. 13 indicate velocity remainder after subtraction of drift velocity from E_rxB_t poloidal rotation velocity. The drift velocity was calculated by the following equation with measured T_e and n_e profile in Fig.12.

$$V_{drift} = \frac{\nabla P}{e n_e B_t} = \frac{k_B T_e}{e B_t}\left(\frac{1}{n_e}\frac{dn_e}{dr} + \frac{1}{T_e}\frac{dT_e}{dr}\right) \tag{4}$$

The blue lines pass the peak of the spectrum in edge region. This indicates negative density gradients mode propagates to ion diamagnetic direction with drift velocity in plasma frame. And the phase velocity changes rapidly in plasma edge making strong velocity shear. However, both calculated E_rxB_t rotation and drift velocity is sensitive the profile of T_e and n_e. The measurements of E_r and more precise profile measurements of T_e and n_e profiles are necessary to confirm this.

The diffusion process is dominated by anomalous one as described in section 4.1. It is likely that convection is dominated by anomalous one as well, because total transport is anomalous one at standard configuration (R_{ax}=3.6m). The fluctuations at positive density

gradient, where particle convection dominates particle transport, will contribute to particle convection and fluctuations in the negative density gradient region, where particle diffusion dominates particle transport, will contribute to particle diffusion. Observed difference of phase velocity indicates difference of underlying mechanisms of two modes.

6. Summary

Systematic studies using density modulation experiments were done to investigate particle transport characteristics at standard magnetic configuration in LHD. The density profiles vary with heating power and B_t. The edge diffusion coefficient is close to gyro-Bohm nature, where fluctuation wavelength around ion Larmor radius play an important role. The diffusion coefficient is larger in the core than at the edge. Particle convection is observed both in core and edge. The core convection velocity shows clear dependence on the T_e gradient. As the temperature gradient is increased, V_{corc} changes direction from inward to outward. This is consistent with the fact that the density profile changes from peaked to hollow with an increase of heating power. However, B_t is also a key parameter to determine V_{corc}. At higher B_t, the core convection reverse direction from inward to outward at larger T_e gradient. The edge convection velocity is inward directed in the most cases. A moderate tendency to decrease V_{edge} with increasing T_e gradient is also observed. The microturbulence measured by PCI shows qualitative correlation between measured spectrum and particle diffusion. Spatial profile of the turbulence measured by 2D PCI shows two different spatial structures. One localizes in positive density gradient region in core, the other localizes in negative density gradient region in edge. The former can contribute to particle convection, the latter can contribute to particle diffusion. More detailed systematic study of particle transport and chracteristics of fluctuation about the density dependence and effect of magnetic configuration is underway and comparison with theoretical models of anomalous transport is planned.

References

[1] K. Narihara et al., Rev. Sci. Instrum., 72 (2001) 1122.
[2] K. Kawahata et al., Rev. Sci. Instrum. **70**, (1999) 707.
[3] K. Tanaka et al., Rev. Sci. Instrum. 75, (2004) 3429.
[4] H. Yamada et al., in 18th Conference Proceedings of Fusion Energy 2000 (Sorrento, Italy 4-10 October 2000) IAEA (2001).
[5] K. Tanaka et al., J. Plasma Fusion Res. Series, 4 (2001) 427.
[6] K.W. Gentle et al., Plasma Phys. Contr. Fusion 29, (1987) 1077.
[7] H.C. Howe, ORNL/TM-11521 (1990).
[8] H. Yamada et al., Plasma Phys. Contrl. Fusion 44 (2002) A245.
[9] S. Murakami et al., Nuclear Fusion 42 (2002) L19-L22.
[10] X. Garbet et al., Phys. Rev. Lett. 91 (2003) 035001-1.
[11] K. Tanaka et al., Rev. Sci. Instrum., Vol 74 (2003) 1633.
[12] A. Sanin et al., Rev. Sci. Instrum. 75, (2004) 3439
[13] L. N. Vyacheslavov et al., to be published 4th Triennial Special Issue of IEEE Transaction on Plasma Science.
[14] S. Kado et al., Jpn. J. Appl. Phys., Part 1 34, (1995) 6492.
[15] C. Michael et al., to be prepared for Rev. Sci. Instrum.
[16] C.D.Beidler et al., Plasma Phys. Contr. Fusion 36, (1994) 317
[17] K.Ida et al., Phys. Rev. Lett. 86 (2001) 5297.

TABLE I: *Effect of toroidal magnetic field B_t on particle diffusion and convection The positive and negative V indicate outward and inward convection respectively.*

Shot	Bt(T)	$D_{edge}(m^2/sec)$	$V_{core}(m/sec)$	$V_{edge}(m/sec)$
48619	1.49	0.43 ± 0.13	5.43 ± 2.89	-2.67 ± 2.87
48672	2.75	0.12 ± 0.004	-2.59 ± 0.45	-3.32 ± 0.28

Figure caption

Fig.1 (a)Electron temperature and (b) density profiles under different NBI heating power. At R_{ax}=3.6m, B_t=2.75T for 2.7 MW and 8.5MW heating, B_t=2.8T for 1MW heating. Temperature profiles are measured by Thomson scattering [1] and density profiles are measured by FIR [2] and CO_2 [3] laser interferometers. Symbols in Fig.1 (a) indicate corresponding chord position of interferometers.

Fig.2 Comparison of modulation amplitude (a) and phase (b) profiles at different heating power. Circular and square symbols indicate measured value, lines indicate calculated values. A 5Hz modulation for 5.2MW and 2Hz modulation for 1MW injection were done.

Fig.3 (a)Estimated particle diffusion coefficients and (b) convection velocities. The dashed lines indicate upper and lower error. The positive and negative V indicate outward and inward convection respectively.

Fig.4 Profiles of electron thermal diffusion coefficients from power balance analysis.

Fig.5 Comparison between experimental values and neoclassical estimation of particle diffusion coefficients

Fig. 6 Electron temperature dependence of particle diffusion coefficients at R_{ax}=3.6m, B_t = 2.75, 2.8T.

Fig.7 The dependence of the convection velocity on electron temperature gradient

Fig. 8 Comparison of (a) electron temperature and (b) density profiles under different toroidal magnetic field.

Fig.9 The dependence of the core convection velocity on electron temperature gradient under different toroidal magnetic field

Fig.10 Comparison of (a) wavenumber and (b) frequency spectrum at different heating power

Fig.11 Measured cross section of phase contrast interferometer
Magnetic flux surfaces are shown every ρ = 0.1 step from ρ = 0.1 to 1.2. Magnetic configuration is standard configuration (R_{ax}=3.6m). The red lines mark the path of CO_2 laser beam.

Fig.12 (a) electron temperature and (b) density profiles during fluctuation measurements by two dimensional phase contrast imaging (2D PCI). Rax=3.6m, Bt=2.75T, NBI heating.

Fig.13 Contour plot of fluctuation power measured by 2D PCI Dark color indicate stronger intensity. The dimension of the intensity is arbitrary unit. Positive and negative ρ indicate bottom and top part of measured position along beam axis in Fig.11 respectively. Positive velocity in top part and negative velocity in bottom part indicate electron diamagnetic direction. Negative velocity in top part and positive velocity in bottom part indicate ion diamagnetic direction. Green lines mark E_rxB_t poloidal rotation velocity and Blue lines show remainder after substraction (∇PxB_t)-diamagnetic drift velocity from E_rxB_t velocity.

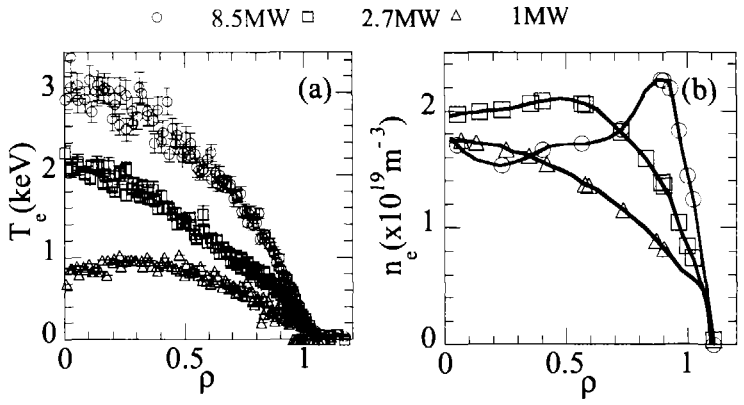

Fig.1

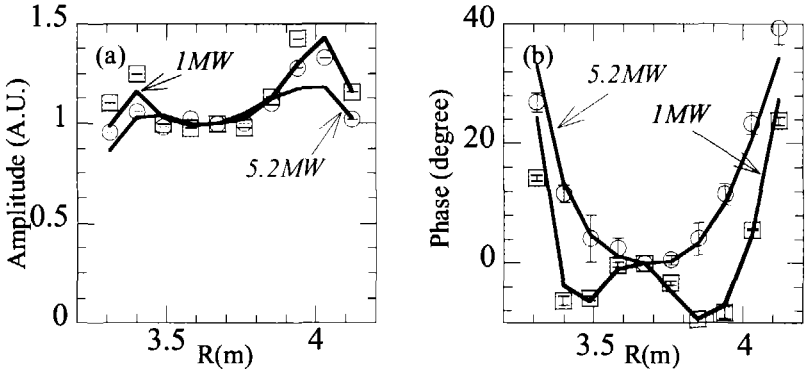

Fig.2

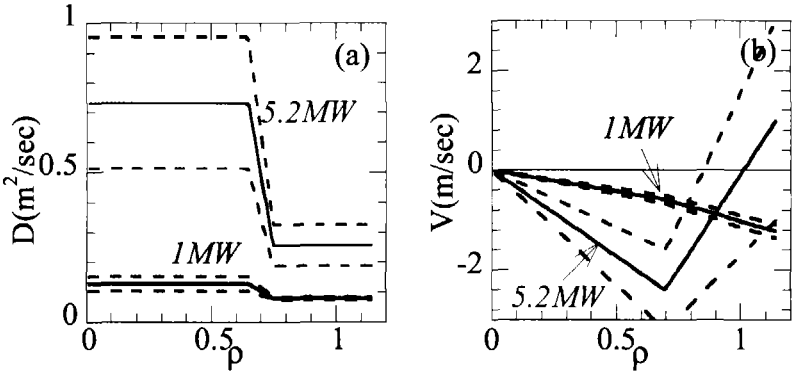

Fig.3

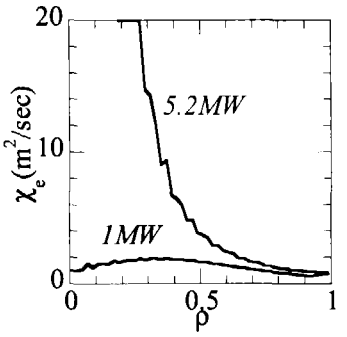

Fig.4

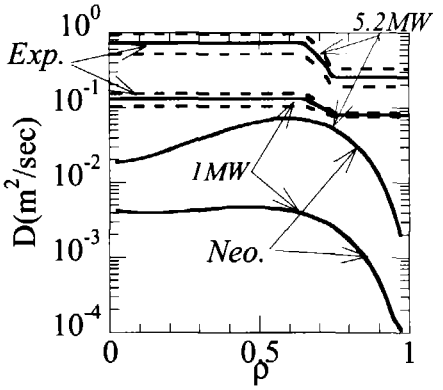

Fig.5

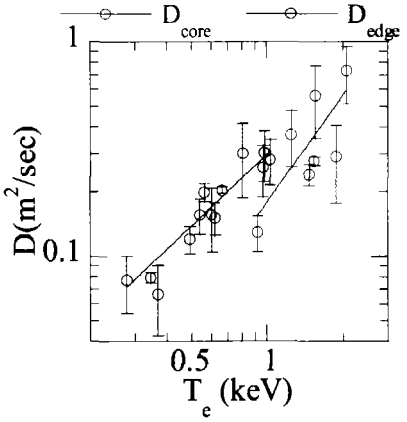

Fig.6

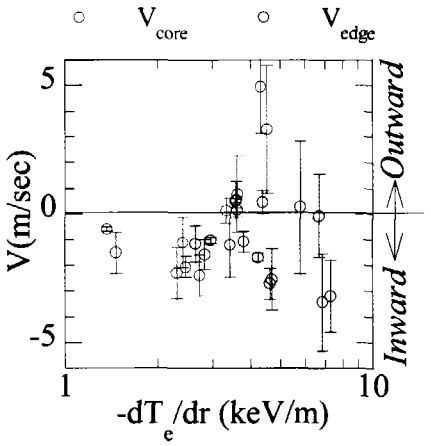

Fig.7

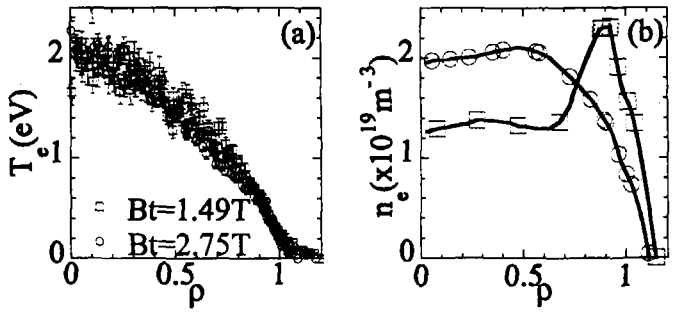

Fig.8

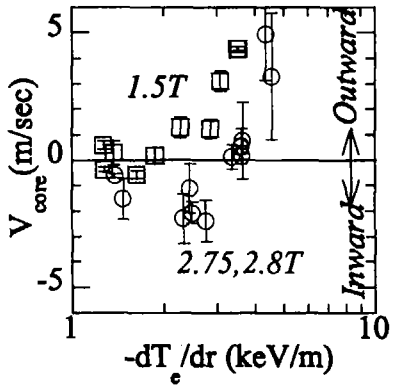

Fig.9

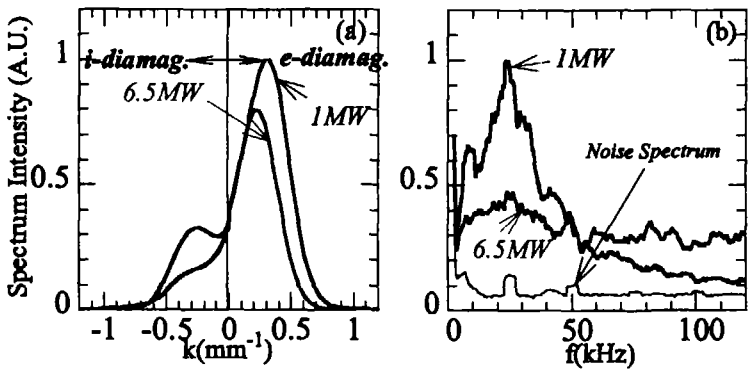

Fig.10

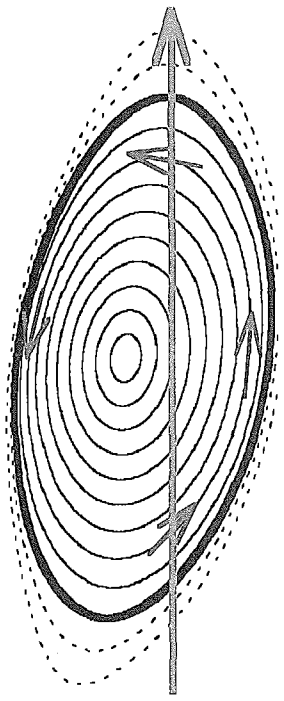

Fig.11

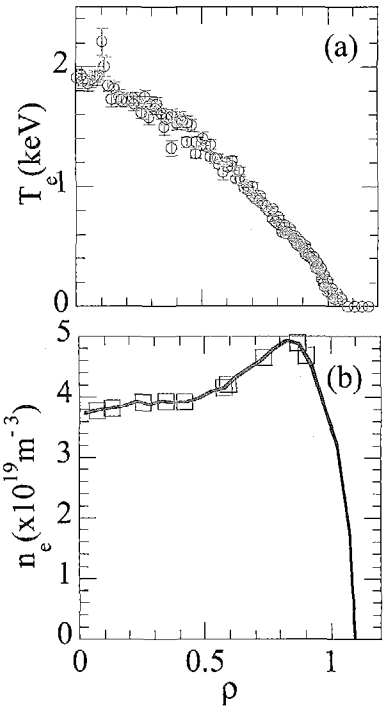

Fig.12

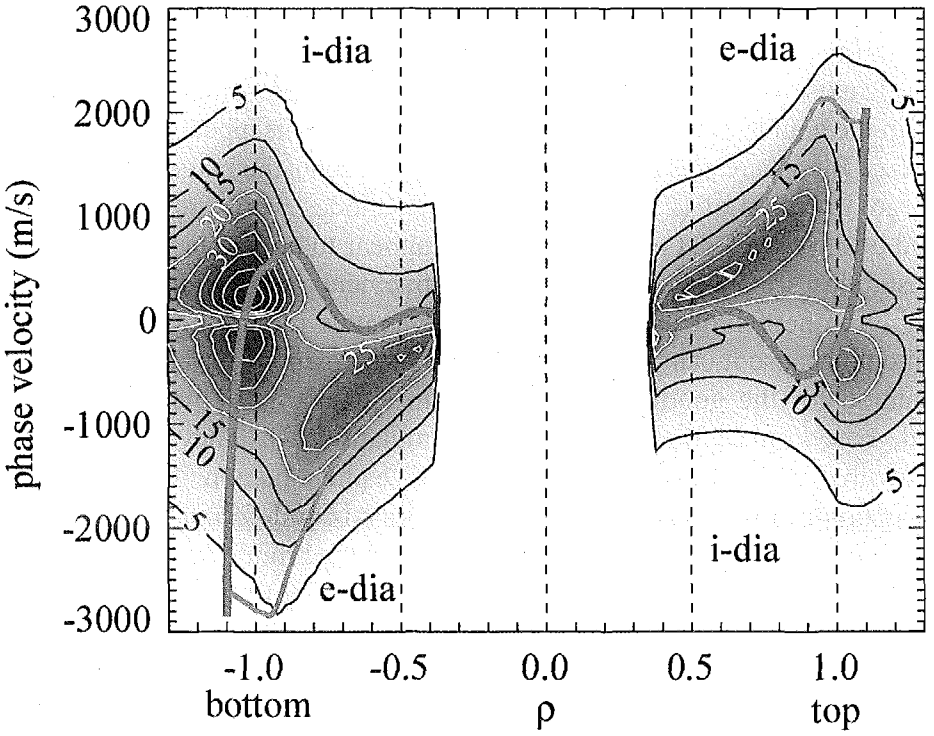

Fig.13